PROCEEDINGS OF SCIENCE

Dark Phase Transition and Gravitational Wave of Strongly Coupled Hidden Sectors

Zhi-Wei Wang[a,b,*]

[a] *School of Physics, The University of Electronic Science and Technology of China, 88 Tian-run Road, Chengdu, China*

[b] *Department of Astronomy and Theoretical Physics, Lund University , SE-223 62 Lund, Sweden*

E-mail: zhiwei.wang@thep.lu.se

We go beyond the state-of-the-art by combining first principal lattice results and effective field theory approaches as Polyakov Loop model to explore the non-perturbative dark deconfinement-confinement phase transition and the generation of gravitational-waves in a dark Yang-Mills theory. We further include fermions with different representations in the dark sector. Employing the Polyakov-Nambu-Jona-Lasinio (PNJL) model, we discover that the relevant gravitational wave signatures are highly dependent on the various representations. We also find a remarkable interplay between the deconfinement-confinement and chiral phase transitions. In both scenarios, the future Big Bang Observer experiment has a higher chance to detect the gravitational wave signals.

41st International Conference on High Energy physics - ICHEP2022
6-13 July, 2022
Bologna, Italy

*Speaker

PoS(ICHEP2022)415

1. Introduction

Dark composite dynamics is particularly interesting since it connects several deep concepts in particle physics such as: non-perturbative physics, dynamical symmetry breaking, UV completion and naturalness. However, (Dark) composite dynamics face challenges to be explored both theoretically and via experiments and thus any extra test is important. In this contribution, we review the results from [1, 2] where we unify first principle lattice simulations and gravitational wave astronomy to constrain the dark sector and provide an alternative test for the dark composite theories. For very recent review, see e.g. [3].

2. Foundation

2.1 What composes the strongly coupled sector?

We construct the strongly coupled sector by using the Dark Yang-Mills theories. We consider two kinds of system in this work: 1. pure gluons 2. gluons with fermions. For pure gluons, it will lead to confinement-deconfinement phase transition. In the case involving fermions, it will lead to either chiral phase transition or confinement-deconfinement phase transition depends on the corresponding fermion representations. In the future work, it might also be interesting to involve scalars as well.

2.2 How to describe the strongly coupled sector?

For pure gluons, there are three well-established effective field theories: 1. Polyakov loop model (PLM) [1, 4, 5]; 2. Matrix Model [6] 3. Holographic QCD model [7].

For system with gluons and fermions, there are also three known effective field theories: 1. Polyakov loop improved Nambu-Jona-Lasinio model (PNJL) [2]; 2. linear sigma model [8]; 3. Polyakov quark meson model [9]. In this work, we will focus on PLM and PNJL.

2.3 Polyakov Loop Model for Pure Gluons

Pisarski first proposed the Polyakov-loop Model as an effective field theory to describe the confinement-deconfinement phase transition of $SU(N)$ gauge theory [10]. In a local $SU(N)$ gauge theory, a global center symmetry $Z(N)$ is used to distinguish confinement phase (unbroken phase) and deconfinement phase (broken phase). An order parameter for the $Z(N)$ symmetry is constructed using the Polyakov Loop (thermal Wilson line) [11]

$$\mathbf{L}(\vec{x}) = \mathcal{P}\exp\left[i\int_0^{1/T} A_4(\vec{x},\tau)\,\mathrm{d}\tau\right]. \tag{1}$$

The symbol $\mathcal{P}$ denotes path ordering and A_4 is the Euclidean temporal component of the gauge field. Here, the Polyakov Loop transforms like an adjoint field under local $SU(N)$ gauge transformations.

It is convenient to define the trace of the Polyakov loop as an order parameter for the $Z(N)$ symmetry

$$\ell(\vec{x}) = \frac{1}{N}\mathrm{Tr}_c[\mathbf{L}], \tag{2}$$

where Tr_c denotes the trace in the colour space. Under a global $Z(N)$ transformation, the Polyakov loop ℓ transforms as a field with charge one

$$\ell \to e^{i\phi}\ell, \qquad \phi = \frac{2\pi j}{N}, \qquad j = 0, 1, \cdots, (N-1) \ . \tag{3}$$

The expectation value of ℓ i.e. $< \ell >$ has the important property:

$$\langle \ell \rangle = 0 \quad (T < T_c, \text{Confined}) \, ; \qquad \langle \ell \rangle > 0 \quad (T > T_c, \text{Deconfined}) \ . \tag{4}$$

At very high temperature, the vacua exhibit a $N-$fold degeneracy:

$$\langle \ell \rangle = \exp\left(i\frac{2\pi j}{N}\right)\ell_0, \qquad j = 0, 1, \cdots, (N-1) \ . \tag{5}$$

where ℓ_0 is defined to be real and $\ell_0 \to 1$ as $T \to \infty$.

2.4 Effective Potential of the Polyakov Loop Model

The simplest effective potential preserving the Z_N symmetry in the polynomial form is [10]

$$\begin{aligned} V_{\mathrm{PLM}}^{(\mathrm{poly})} &= T^4\left(-\frac{b_2(T)}{2}|\ell|^2 + b_4|\ell|^4 + \cdots - b_3\left(\ell^N + \ell^{*N}\right)\right) \\ \text{where} \quad b_2(T) &= a_0 + a_1\left(\frac{T_0}{T}\right) + a_2\left(\frac{T_0}{T}\right)^2 + a_3\left(\frac{T_0}{T}\right)^3 + a_4\left(\frac{T_0}{T}\right)^4, \end{aligned} \tag{6}$$

where "$\cdots$" represent any required lower dimension operator than ℓ^N and the a_i, b_i coefficients in $V_{\mathrm{PLM}}^{(\mathrm{poly})}$ are determined by fitting the lattice results.

2.5 Including Fermions

The Polyakov-loop-Nambu-Jona-Lasinio (PNJL) model is used to describe phase-transition dynamics in dark gauge-fermion sectors [12]. The finite-temperature grand potential of the PNJL models can be generically written as

$$V_{\mathrm{PNJL}} = V_{\mathrm{PLM}}[\ell, \ell^*] + V_{\mathrm{cond}}\left[\langle\bar{\psi}\psi\rangle\right] + V_{\mathrm{zero}}\left[\langle\bar{\psi}\psi\rangle\right] + V_{\mathrm{medium}}\left[\langle\bar{\psi}\psi\rangle, \ell, \ell^*\right] \ , \tag{7}$$

where $V_{\mathrm{PLM}}[\ell, \ell^*]$, $V_{\mathrm{cond}}\left[\langle\bar{\psi}\psi\rangle\right]$ and $V_{\mathrm{zero}}\left[\langle\bar{\psi}\psi\rangle\right]$ denotes respectively the Polyakov loop model potential (discussed above), the condensate energy and the fermion zero-point energy. The medium potential $V_{\mathrm{medium}}\left[\langle\bar{\psi}\psi\rangle, \ell, \ell^*\right]$ encodes the interactions between the chiral and gauge sector which arises from an integration over the quark fields coupled to a background gauge field.

3. Bubble Nucleation and Gravitatioanl Wave

3.1 Bubble Nucleation

Confinement-deconfinement phase transition

The confinement-deconfinement phase transition applies to the pure gluon case. In a first-order phase transition, the transition occurs via bubble nucleation and it is essential to compute the

nucleation rate. The tunnelling rate due to thermal fluctuations from the metastable vacuum to the stable one is suppressed by the three-dimensional Euclidean action $S_3(T)$

$$\Gamma(T) = T^4 \left(\frac{S_3(T)}{2\pi T}\right)^{3/2} e^{-S_3(T)/T}\,, \tag{8}$$

where the three-dimensional Euclidean action reads (for the pure gluon case)

$$S_3(T) = 4\pi T \int_0^\infty \mathrm{d}r'\, r'^2 \left[\frac{1}{2}\left(\frac{\mathrm{d}\ell}{\mathrm{d}r'}\right)^2 + V'_{\rm eff}(\ell, T)\right]\,. \tag{9}$$

Note that here $[\ell] = 0$, I thus convert the radius into a dimensionless quantity $r' = r\,T$.

The bubble profile (instanton solution) is obtained by solving the E.O.M. of the $S_3(T)$

$$\frac{\mathrm{d}^2\ell(r')}{\mathrm{d}r'^2} + \frac{2}{r'}\frac{\mathrm{d}\ell(r')}{\mathrm{d}r'} - \frac{\partial V'_{\rm eff}(\ell, T)}{\partial \ell} = 0\,, \tag{10}$$

where the boundary conditions (deconfinement $\to$ confinement) are

$$\frac{\mathrm{d}\ell(r'=0,T)}{\mathrm{d}r'} = 0\,, \qquad\qquad \lim_{r'\to 0}\ell(r', T) = 0\,. \tag{11}$$

We used the method of overshooting/undershooting (`Python` package).

Chiral Phase Transition The chiral phase transition applies to the case when fermions under the fundamental representations are involved. We use the chiral condensate $\sigma \propto \langle\bar{\psi}\psi\rangle$ as the order parameter. In this case, the procedure to obtain the bubble profile is similar to the above discussions. However, the boundary conditions Eq. (11) need to be changed accordingly since chiral phase transition do not possesses the characteristics of symmetry non-restoration.

3.2 Gravitational-wave spectrum

Contributions to the gravitational wave spectrum from bubble collision and turbulence are subleading and thus we focus on the sound wave. The GW spectrum from sound waves is given by

$$h^2\Omega_{\rm GW}(f) = h^2\Omega_{\rm GW}^{\rm peak}\left(\frac{f}{f_{\rm peak}}\right)^3\left[\frac{4}{7} + \frac{3}{7}\left(\frac{f}{f_{\rm peak}}\right)^2\right]^{-\frac{7}{2}}\,, \tag{12}$$

where the peak frequency writes

$$f_{\rm peak} \simeq 1.9\cdot 10^{-5}\,\mathrm{Hz}\left(\frac{g_*}{100}\right)^{\frac{1}{6}}\left(\frac{T}{100\,\mathrm{GeV}}\right)\left(\frac{\tilde{\beta}}{v_w}\right)\,, \tag{13}$$

and the peak amplitude writes

$$h^2\Omega_{\rm GW}^{\rm peak} \simeq 2.65\cdot 10^{-6}\left(\frac{v_w}{\tilde{\beta}}\right)\left(\frac{\kappa_{sw}\,\alpha}{1+\alpha}\right)^2\left(\frac{100}{g_*}\right)^{\frac{1}{3}}\Omega_{\rm dark}^2\,, \tag{14}$$

where α, β, v_w and κ_{sw} denote respectively the strength parameter, the inverse duration, wall velocity and the efficiency factor. Note that the factor $\Omega_{\rm dark}^2$ accounts for the dilution of the GWs by the non-participating SM d.o.f.

$$\Omega_{\rm dark} = \frac{\rho_{\rm rad,dark}}{\rho_{\rm rad,tot}} = \frac{g_{*,\rm dark}}{g_{*,\rm dark} + g_{*,\rm SM}}\,. \tag{15}$$

In Fig. 1, I present the GW spectrum for arbitrary N in the pure gluon case. It is interesting to see that for $N = 6$, it provides the strongest gravitational wave signals and future gravitational wave detectors as BBO and DECIGO have a better chance to detect the signals.

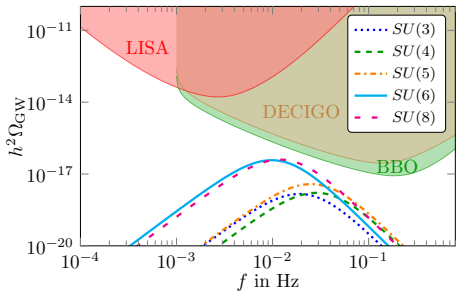

Figure 1: The dependence of the GW spectrum on the number of dark colours is shown for the values $N = 3,4,5,6,8$. All spectra are plotted with the bubble wall velocity set to the Chapman-Jouguet detonation velocity and with Tc= 1 GeV.

Rep.	flavour	chiral PT	conf.-deconf.
Fund.	3	1st	X
adjoint	1	2nd	1st
2-index Sym.	1	2nd	1st

Table 1: Representations versus different phase transitions. X denotes no phase transition.

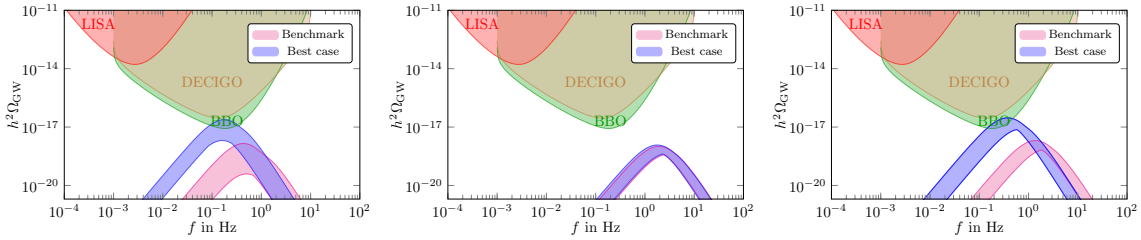

Figure 2: GW spectra of the chiral/confinement phase transition of SU(3) with $N_f = 3$ fundamental quarks (left), $N_f = 1$ adjoint quarks (middle), and $N_f = 1$ two-index symmetric quarks (right) for a benchmark scenario and the best-case scenario in the parameter space. Figures taken from [2].

3.3 Representation Matters

In Tab. 1, I present for different group representations, their corresponding phase transitions (chiral or confinement-deconfinement) and the order (first or second). Their corresponding GW spectra are displayed in Fig. 2. We observe that the one flavour two-index symmetric representation case provides the strongest gravitational wave signals. It is also interesting to notice that compared to the pure gluon case, adjoint quarks suppress the GW signal while two-index symmetric quarks enhance it. In Fig. 3, I present the signal to noise ratio (SNR) as a function of the critical temperature for different representations. We observe that SNR varies with respect to different representations and the one flavour two-index symmetric representation case provides the biggest SNR consistent with the results shown in Fig. 2.

Acknowledgments Z.-W. Wang thanks W.C. Huang, R. Pasechnik, M. Reichert, F. Sannino, and C. Zhang for joint work on the topics discussed above. Z.- W. W. is partially supported by the Swedish Research Council grant, contract number 2016-05996, and the European Research Council

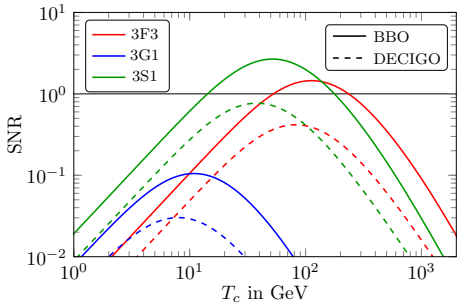

Figure 3: Signal-to-noise ratio as a function of the critical temperature for the best-case scenarios of each model at BBO and DECIGO with an observation time of 3 years.

(ERC) under the European Union's Horizon 2020 research and innovation program (No. 668679).

References

[1] W. C. Huang, M. Reichert, F. Sannino and Z. W. Wang, Phys. Rev. D **104** (2021) 035005 [arXiv:2012.11614 [hep-ph]].

[2] M. Reichert, F. Sannino, Z. W. Wang and C. Zhang, JHEP **01** (2022), 003 [arXiv:2109.11552 [hep-ph]].

[3] M. Reichert and Z. W. Wang, [arXiv:2211.08877 [hep-ph]].

[4] Z. Kang, J. Zhu and S. Matsuzaki, JHEP **09** (2021), 060 [arXiv:2101.03795 [hep-ph]].

[5] P. Carenza, R. Pasechnik, G. Salinas and Z. W. Wang, [arXiv:2207.13716 [hep-ph]].

[6] J. Halverson, C. Long, A. Maiti, B. Nelson and G. Salinas, JHEP **05** (2021), 154 [arXiv:2012.04071 [hep-ph]].

[7] F. R. Ares, O. Henriksson, M. Hindmarsh, C. Hoyos and N. Jokela, Phys. Rev. D **105** (2022) no.6, 066020 [arXiv:2109.13784 [hep-th]].

[8] A. J. Helmboldt, J. Kubo and S. van der Woude, Phys. Rev. D **100** (2019) no.5, 055025 [arXiv:1904.07891 [hep-ph]].

[9] B. J. Schaefer, J. M. Pawlowski and J. Wambach, Phys. Rev. D **76** (2007), 074023 [arXiv:0704.3234 [hep-ph]].

[10] R. D. Pisarski, Phys. Rev. D **62** (2000), 111501 [arXiv:hep-ph/0006205 [hep-ph]].

[11] A. M. Polyakov, Phys. Lett. B **72** (1978), 477-480

[12] K. Fukushima and V. Skokov, Prog. Part. Nucl. Phys. **96** (2017), 154-199 [arXiv:1705.00718 [hep-ph]].